Current Research in Food Science 4 (2021) 270–278

Contents lists available at ScienceDirect

Current Research in Food Science

journal homepage: www.editorialmanager.com/crfs/

Research Paper

Adsorption and foaming properties of edible egg yolk peptide nanoparticles: Effect of particle aggregation

Mengyue Xu [a,1], Zhenya Du [a,1], Huanyin Liang [a], Yunyi Yang [a], Qing Li [a], Zhili Wan [a,b,c,*], Xiaoquan Yang [a]

[a] Laboratory of Food Proteins and Colloids, School of Food Science and Engineering, Guangdong Province Key Laboratory for Green Processing of Natural Products and Product Safety, South China University of Technology, Guangzhou, 510640, China
[b] Overseas Expertise Introduction Center for Discipline Innovation of Food Nutrition and Human Health (111 Center), Guangzhou, 510640, China
[c] Department of Chemistry, The Chinese University of Hong Kong, Shatin, N. T., Hong Kong, China

ARTICLE INFO

Keywords:
Edible foams
Egg yolk peptide nanoparticles
Peptide self-assembly
Particle aggregates
Pickering stabilization

ABSTRACT

The adsorption and foaming properties of an edible colloidal nanoparticle (EYPNs), self-assembled from the food-derived, amphiphilic egg yolk peptides, were investigated, with the aim of evaluating their potential as efficient particulate stabilizers for development of aqueous food foams. The influence of particle aggregation induced by the changes of environmental conditions (mainly the pH) on these properties of EYPN systems was determined. Our results showed that the EYPNs are a highly pH-responsive system, showing the pH-dependent particle aggregation behavior, which is found to strongly affect the interfacial adsorption and macroscopic foaming behaviors of systems. Compared to high pH (6.0–9.0), the EYPNs at low pH (2.0–5.0) showed higher surface activity with a lower equilibrated surface tension as well as a higher packing density of particles and particle aggregates at the interface, probably due to the reduced electrostatic adsorption barrier. Accordingly, the EYPNs at these low pH values exhibited significantly higher foamability and foam stability. The presence of large particle clusters and/or aggregates formed at low pH in the continuous phase may contribute to the foam stability of EYPNs. These results indicate that our edible peptide-based nanoparticle EYPNs can be used as a new class of Pickering-type foam stabilizer for the design of food foams with controlled material properties, which may have sustainable applications in foods, cosmetics, and personal care products.

1. Introduction

Aqueous foams are widely used in many fields, ranging from food, cosmetics, and health care products to industrial applications like enhanced oil recovery or flotation (Cantat et al., 2013; Rio et al., 2014). Controlling the foam properties including foamability and foam stability is crucial and also challenging for practical material applications, since aqueous foams are thermodynamically unstable systems and have complex structures at multiple length scales (Rio et al., 2014; Gonzenbach et al., 2006). The formation and stabilization of foams strongly depend on the type and properties of the foaming agents. Particles have been demonstrated to be one of the most attractive foaming agents due to their strong and irreversible adsorption at the air-water interface and thus the high foam stability based on Pickering mechanism (Gonzenbach et al., 2006; Binks, 2002; Binks and Horozov, 2005). Many types of colloidal particles such as inorganic silica (Binks and Horozov, 2005; Du et al., 2003; Dickinson et al., 2004), alumina (Gonzenbach et al., 2006), latexes (Binks et al., 2007), and graphene (Zhang et al., 2019), as well as organic polymeric particles and microrods (Fujii et al., 2006; Alargova et al., 2004), have been used as particulate foam stabilizers to make Pickering-type foams. In recent years, considering the environmental drawbacks and even the potential safety concerns of synthetic particles, there is a growing interest in the development of food-grade aqueous foams by using the edible particles as foam stabilizers, such as particles made of animal and plant proteins (Wan, Yang and Sagis, 2016a; Zou et al., 2016; Peng et al., 2018; Li et al., 2020; Schmitt et al., 2007), modified starch (Asghari et al., 2016), cellulose (Cervin et al., 2013), and calcium carbonate (Cui et al., 2010; Binks et al., 2017).

* Corresponding author. Laboratory of Food Proteins and Colloids, School of Food Science and Engineering, Guangdong Province Key Laboratory for Green Processing of Natural Products and Product Safety, South China University of Technology, Guangzhou, 510640, China.
E-mail address: zhiliwan@scut.edu.cn (Z. Wan).
[1] These authors contributed equally to this work.

https://doi.org/10.1016/j.crfs.2021.04.002
Received 28 January 2021; Received in revised form 3 April 2021; Accepted 6 April 2021

Generally, an efficient foaming formulation should be able to adsorb rapidly and readily at the interface leading to high foamability, and subsequently provide high stability of the foam by forming an irreversibly adsorbed elastic surface layer. However, it remains difficult for a foam stabilizer to have both superior foamability and the resultant foam stability, since they are often counteracting features. For example, colloidal particles allow the formation of the so-called Pickering foams with a long lifetime by forming a particle-laden solid-like bubble interface (Gonzenbach et al., 2006; Binks and Horozov, 2005; Du et al., 2003); however, most of the bare particles exhibit a poor foamability producing a limited amount of foam, mainly due to their slow adsorption dynamic as well as the high adsorption barriers. In order to use the solid particles to effectively stabilize bubbles and foams, these particles have to be modified chemically or through the physical adsorption of oppositely charged surfactants (Gonzenbach et al., 2006; Cui et al., 2010; Binks et al., 2017; Maestro et al., 2014; Binks et al., 2008; Arriaga et al., 2012). There are many examples of the particle-surfactant combinations used for the preparation of aqueous foams, such as the mixtures of silica particles with cationic di-C_{10}DMAB (di-decyldimethyl-ammonium bromide) or n-amylamine (Maestro et al., 2014; Binks et al., 2008), and $CaCO_3$ particles with anionic sodium dodecyl sulphate (SDS) (Cui et al., 2010). Compared to the raw inorganic particles, the food protein-based colloidal particles are more surface-active and thus have higher affinities at liquid interfaces due to the typical amphiphilic structure of protein molecules. For example, particles made from soy protein, zein, gliadin, whey protein and egg white protein have shown to give Pickering-type stability of aqueous foams (Wan, Yang and Sagis, 2016a; Zou et al., 2016; Peng et al., 2018; Li et al., 2020; Schmitt et al., 2007; Matsumiya and Murray, 2016; Dombrowski et al., 2016). However, these natural macromolecular proteins, especially the complex plant proteins, are often restricted by relatively poor solubility, large particle size, and uncontrollable particle wettability, and thus require complicated and time-consuming particle fabrication as well as surface modification processes (Wan, Yang and Sagis, 2016a; Zou et al., 2016; Peng et al., 2018; Matsumiya and Murray, 2016; Wan et al., 2015), which limit their practical use as efficient foam stabilizers to make aqueous foams. In this field, the design and fabrication of new edible protein particles with suitable colloidal properties (e.g., particle size and wettability) is still highly desired for the efficient production of food-grade foams when considering their safe applications in the food, pharmaceutical, and personal care products.

Recently, we reported that the food-derived, amphiphilic egg yolk peptides (EYPs) can be used to create edible colloidal nanoparticles via the "bottom-up" self-assembly approach (Du et al., 2019). The amphiphilic EYPs are prepared by the controlled enzymatic hydrolysis of purified defatted egg yolk protein, a by-product obtained after lecithin extraction from egg yolk. These EYPs are found to be able to self-assemble into spherical micellar nanoparticles (EYPNs) mainly through the hydrophobic interactions, when the concentration of EYPs in aqueous solution is higher than their critical micelle concentration (CMC) of 0.1 mg/mL (Du et al., 2019). We showed that these natural peptide-based nanoparticles have many advantages in the stabilization of particle-laden liquid interfaces, such as their small particle size (around 25 nm in diameter), intermediate wettability, satisfactory interfacial activity, and structural deformability at the oil-water interface. Accordingly, these interesting EYPNs can be used as an efficient particulate emulsifier to prepare stable food-grade Pickering nanoemulsions (droplet diameter below 200 nm) due to the irreversible and compact adsorption of intact EYPNs at the droplet surfaces (Du et al., 2019). This finding demonstrates the capacity of edible EYPNs as a new class of particulate stabilizer for production of Pickering-type food emulsions and foams.

Considering the suitable colloidal properties of EYPNs and their promising applications in the development of food foams and emulsions, it is therefore of interest to further study the adsorption of edible EYPNs at the air-water interface as well as the corresponding foaming characteristics. Herein, we aim to evaluate the potential of the peptide-based nanoparticle EYPNs as an edible foam stabilizer to prepare food aqueous foams. Previous studies have shown that the surface and foaming behaviors of protein-based particles generally depend on processing environmental conditions such as pH, temperature, and ionic strength, which could change the size and surface charge of protein particles (Wan, Yang and Sagis, 2016a; Peng et al., 2018; Dombrowski et al., 2016). We therefore investigated the impact of environmental conditions (e.g., pH and salt concentration) on the interfacial adsorption and foaming properties of EYPNs. Their structural properties including particle size, surface charge, and microstructure were first characterized. Subsequently, the foamability, foam stability, as well as bubble microstructure of EYPN-stabilized aqueous foams were determined.

2. Materials and methods

2.1. Materials

Lecithin-free egg yolk protein was kindly provided by Guangzhou Hanfang Pharmaceutical, China. The protein sample was further purified using Milli-Q water (18.2 MΩ cm) and 95% ethanol alternatively three times under mild agitation, to remove the residual lipids and impurities. The ratios of protein to solvent were 1:3 (v/v) and 1:5 (v/v) for ethanol and water, respectively. The purified protein was isolated, lyophilized, and then stored at −20 °C for further use. The protein content of purified sample was 90.7% according to the micro-Kjeldahl method (N × 6.25, dry basis). Trypsin (250 U/mg) was purchased from Novozymes, Denmark. Nile Blue A was purchased from Sigma-Aldrich (St. Louis, MO). All other chemicals used were of analytical grade.

2.2. Preparation of amphiphilic egg yolk peptides (EYPs) and EYP nanoparticles (EYPNs)

EYPs and EYPNs were prepared according to our previous method (Du et al., 2019). In brief, the suspension of purified egg yolk protein (4 wt%) was made by dispersing the protein in Milli-Q water. The pH of the suspension was adjusted to pH 8.0 using 1 M NaOH solution, followed by adding trypsin with a weight ratio of 1:100. The resulting mixture (pH 8.0) was incubated at 40 °C for 180 min with continuous stirring to hydrolyze the protein. After that, the amphiphilic EYP solution was obtained and then passed through a 0.45 μm filter. Based on our previous study (Du et al., 2019), the self-assembled micellar EYPNs can be formed when the concentration of EYPs is higher than their critical micelle concentration (CMC, around 0.1 mg/mL). The pH of the mixtures was adjusted to pH 7.0, and then the hydrolysis process was terminated by placing them into boiling water for 15 min. The hydrolyzed sample was centrifuged twice at 8000 g for 20 min, and the supernatant was passed through a 0.45 μm filter and dialyzed (MWCO 100 Da) against water at 4 °C for 48 h before freeze-drying. The lyophilized powder was stored at −20 °C for further use.

2.3. Preparation of EYPN-stabilized aqueous foams

EYPN solution was prepared by dissolving lyophilized powder in water in sealed glass vials (2.5 cm internal diameter, 9 cm height) under mild agitation to obtain a clear solution. The aqueous foams were prepared by shearing and aerating the EYPN solution using an ultraturrax (IKA T10 basic) at 20,000 rpm for 2 min, and then the obtained foams were left to decay at room temperature (25 °C). Foam heights were measured using a ruler, and the foam overrun was calculated by using equation: overrun (%) = $[(V_t - V_0)/V_0] \times 100$, where V_t is the total volume of the foam and V_0 is the initial liquid volume. The dried foam samples were prepared by air-drying in oven at 25 °C for 24 h, or by freeze-drying for 24 h in a Christ DELTA 1–24 LSC freeze-dryer (Christ, Germany).

2.4. Particle size and zeta potential

The particle size and zeta potential of EYPN suspensions (0.1 and 1 wt %, ~10 and 100 times above the CMC of EYPs, respectively) were determined using a Nano ZS Zetasizer (Malvern Instruments Ltd, UK), after appropriate dilutions to avoid the effect of multiple scattering. All measurements were carried out at 25 °C, and the results reported are averages of three measurements.

2.5. Dynamic adsorption of EYPNs at the air-water interface

The dynamic surface tension of EYPNs (0.1 and 1 wt%) at the air-water interface was determined using a pendant drop method (OCA-20, Dataphysics Instruments GmbH, Germany). A drop of sample solution (10 μL) was formed in an optical glass cuvette, monitored with a video camera, and allowed to stand for 180 min to achieve adsorption at the interface. The cuvette was partially filled with the solution to saturate the air surrounding the drop and sealed with a Parafilm M laboratory film, which could reduce the sample evaporation. The surface tension (γ) was calculated from the shape analysis of pendent drop according to the Young-Laplace equation. The surface pressure is $\Pi = \gamma_0 - \gamma(t)$, where γ_0 is the surface tension of phosphate buffer (10 mM, pH 7.0) and $\gamma(t)$ is the time-dependent surface tension of the tested samples. All measurements were performed at 25 °C, and reported values represent the average of 3–5 measurements.

2.6. Three-phase contact angle

The air-in-water three-phase contact angle of EYPNs was determined using the sessile drop method on an OCA-20 optical contact angle meter (Dataphysics Instruments GmbH, Germany). The EYPN powder pellets were prepared and then placed into an optical glass cuvette. A drop of Milli-Q water (5 μL) was deposited on the pellet surface through a high-precision syringe. The drop image was photographed using a high-speed video camera and then contact angles were determined automatically with a Laplace-Young fit. Measurements were performed on at least three droplets for each pellet, and five pellets for each sample were measured.

2.7. Atomic force microscopy (AFM)

A droplet of EYPN suspension (0.1 wt%) was placed on freshly cleaved mica and dried in air. AFM images were acquired in the ScanAsyst mode under ambient conditions using silicon nitride tips (Bruker, USA). A MultiMode 8 Scanning Probe Microscope (Bruker, USA) was employed for AFM observations.

2.8. Confocal laser scanning microscopy (CLSM)

CLSM observations were performed with a Leica TCS SP5 confocal microscope. The EYPN suspension (1 wt%) and the nanoparticles used for making foams were labelled with Nile Blue A (0.01 wt%), which was first dissolved in EYPN solutions prior to the sample preparation. The stained fresh samples were placed on concave confocal microscope slides and examined using a helium neon laser (He/Ne) with excitation at 633 nm. The EYPNs dyed with Nile Blue is green in the images.

2.9. Field emission scanning electron microscopy (FE-SEM)

A Zeiss Merlin field emission scanning electron microscope was used to observe the microstructures of the dried EYPN foams. The dried samples were carefully transferred and adhered on a holder and then sputter-coated with gold (JEOL JFC-1200 fine coater, Japan) before imaging.

2.10. Statistical analysis

Unless specified in our experiments, at least three freshly prepared samples were characterized. Analysis of variance (ANOVA) of the data was performed using the SPSS 19.0 statistical analysis software. Duncan's test was used for comparison of mean values among samples using a level of significance of 5%.

3. Results and discussion

Our previous study has shown that the edible peptide nanoparticles, EYPNs, prepared through the "bottom-up" self-assembly of amphiphilic EYPs, have many interesting colloidal properties including small particle size, intermediate wettability, high interfacial activity, as well as structural deformability at the oil-water interface, and thus can be used as an efficient particulate emulsifier to prepare stable food-grade Pickering nanoemulsions (Du et al., 2019). Herein, in this study, we further investigated the adsorption of EYPNs at the air-water interface and then evaluate their foaming characteristics, with the aim of expanding the promising applications of peptide-based nanoparticles in the development of edible food colloids.

3.1. Particle aggregation behavior of EYPN dispersions

Since the environmental conditions such as pH and ionic strength often obviously change the size and surface charge of protein/peptide particles, which can affect the surface and foaming properties of systems, the effects of the changes of pH (2.0–9.0) and NaCl concentrations (0–500 mM) on the particle size, zeta potential, and microstructure of EYPNs were evaluated. As can be seen, at and above pH 7.0, the aqueous dispersions of EYPNs are transparent and homogeneous with the volume-weighted average diameter of around 25 nm (Fig. 1a and b). Results of zeta potential show that these nanoparticles within this pH range (7.0–9.0) are highly negatively charged (−30.2~−41.7 mV), which thus endows EYPN dispersions with effective colloidal stability by electrostatic repulsion (Fig. 1c). However, particle flocculation and aggregation began to appear at and below pH 6.0, and the extent of aggregation increased with decreasing pH values, especially at higher particle concentration (1 wt%, Fig. 1a). Furthermore, the aqueous EYPN dispersions within this pH range of 2.0–4.0 showed evident phase separation and sedimentation after 24 h storage at 25 °C (data not shown). This can be explained by the fact that the surface charge of EYPNs was gradually reduced with decreasing pH values (Fig. 1c), and accordingly, the Coulomb repulsion forces in systems are insufficient to counteract the long-range hydrophobic attractions between the EYPNs (Du et al., 2019), which thus bring these nanoparticles together and leading to the formation of large particle clusters and/or aggregates.

The influence of NaCl addition (0–500 mM) on the particle size and zeta potential values of EYPN dispersions was further investigated. As expected, the presence of NaCl led to the decreased surface charge of EYPNs due to the salt-induced electrostatic shielding (Fig. 1d). Generally, the increase of ionic strength can reduce the electrostatic repulsion, which thus results in the increased extent of particle aggregation. As seen from Fig. S1, when the NaCl concentration was more than 200 mM, a significant size increase of EYPNs can be observed due to the insufficient repulsion forces in systems (Fig. 1d). However, it is noted that the EYPN dispersions (1 wt%) remained relatively stable within the whole range of NaCl concentration applied without obvious phase separation and sedimentation in sample appearance (inset image of Fig. 1d). The satisfactory stability of EYPNs towards ionic strength may be due to their heterogeneous internal structure (Du et al., 2019), which could reduce the effect of salt ions on the interactions among particles and therefore to some extent prevent the particle aggregation (Dai et al., 2017; Shen et al., 2020).

The microstructures of EYPNs at different pHs were then determined by using AFM and CLSM, and the results are shown in Figs. 2 and 3,

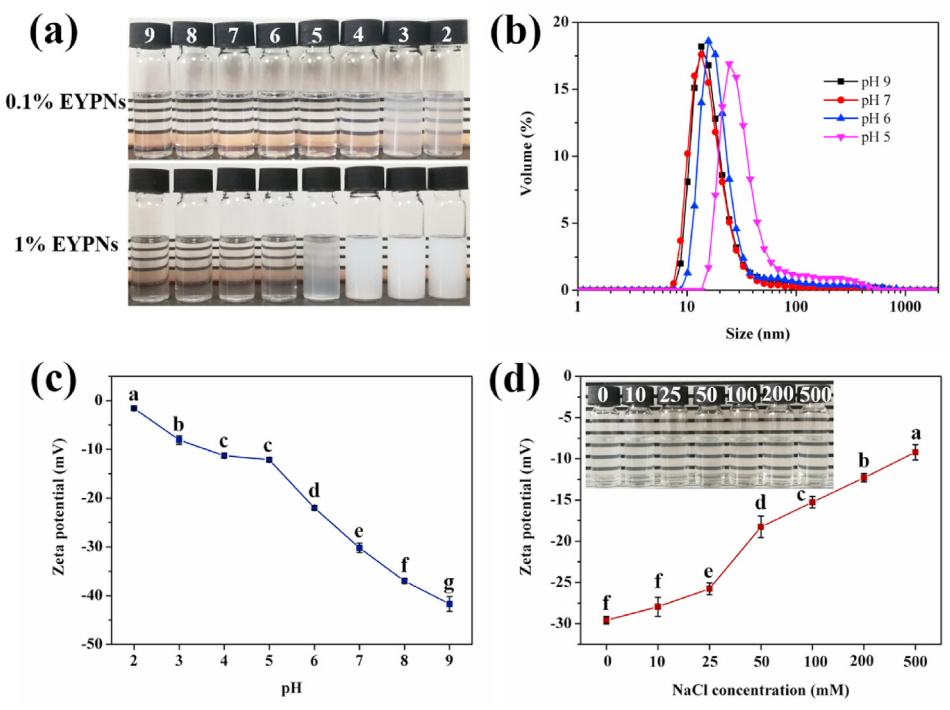

Fig. 1. (a) Photographs of EYPN dispersions (0.1 and 1 wt%) freshly prepared at different pHs (2.0–9.0). (b) Particle size distributions of these EYPNs at different pHs (pH 6.0–9.0: 1 wt% EYPNs; pH 5.0: 0.1 wt% EYPNs). (c and d) Zeta potential of 1 wt% EYPNs prepared at different pHs (c, without NaCl) or with different NaCl concentrations (d, at pH 7.0). Inset image in (d) shows the photograph of 1 wt% EYPN dispersions (pH 7.0) with different NaCl concentrations (0–500 mM). Note: Different letters in each data indicate significant differences between groups ($p < 0.05$).

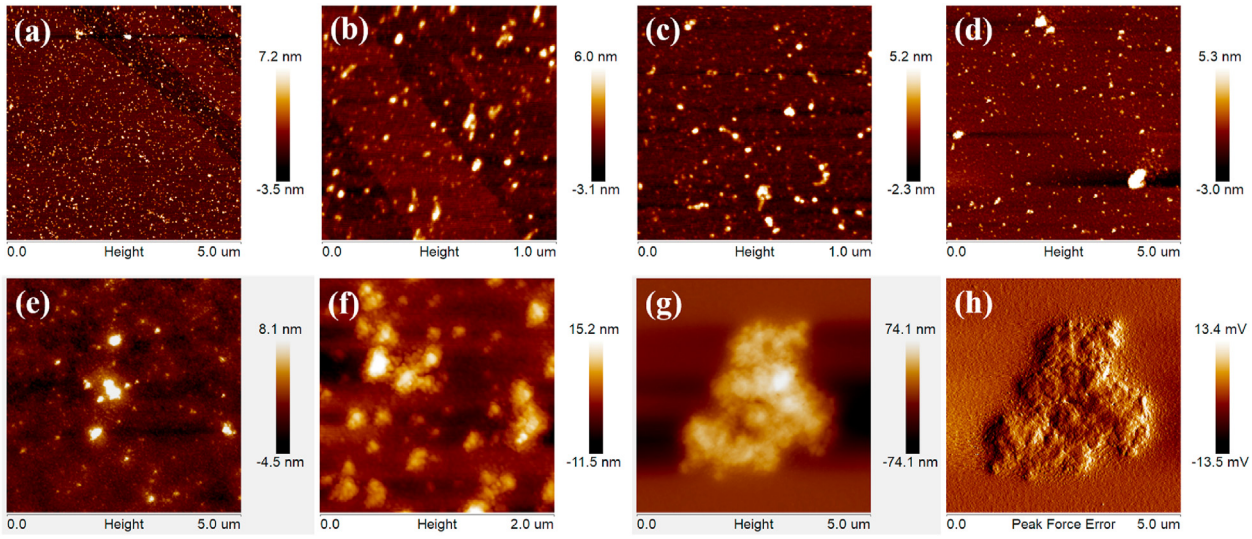

Fig. 2. AFM height (a–g) and corresponding peak force error (h) images of the 0.1 wt% EYPN dispersions obtained at different pHs: (a and b) pH 9.0; (c) pH 7.0; (d) pH 5.0; (e) pH 4.0; (f) pH 3.0; (g and h) pH 2.0.

respectively. At pH 7.0 and 9.0, the EYPNs showed a well-dispersed spherical morphology with a relatively uniform size distribution (Fig. 2a–c), which is in good agreement with the result of particle size distribution (Fig. 1b) as well as our previous study (Du et al., 2019). However, at and below pH 5.0, large particle aggregates were clearly observed, and the aggregation extent became more apparent with the decrease of pH values (Fig. 2d–h). We then prepared the Nile Blue-labelled EYPNs (1 wt%) to further observe the aggregated particle structures at low pH values (2.0–5.0), and these obtained CLSM images clearly confirm the formation of larger particle clusters and aggregates (Fig. 3). These microstructure observations are in good agreement with the abovementioned appearance and zeta potential results (Fig. 1a and c) of EYPN dispersions. This means that as food peptide-based nanoparticles, the EYPNs are a highly pH-responsive system, and their aggregation behaviors in aqueous solutions strongly depend on the pH changes, which are expected to have a significant impact on the interfacial adsorption and subsequent foaming properties of systems (Wan, Yang, & Sagis, 2016a, 2016b).

3.2. Adsorption and interfacial wettability of EYPNs at the air-water interface

The time evolution of surface tension (γ) of EYPNs (0.1 and 1 wt%) was first determined to study their adsorption behavior at the air-water interface, and the results are shown in Fig. 4a and b. As can be seen, for all investigated cases, the surface tension values initially decreased rapidly with adsorption time, and after 3 h they became relatively constant as the surfaces were already saturated. This suggests that small

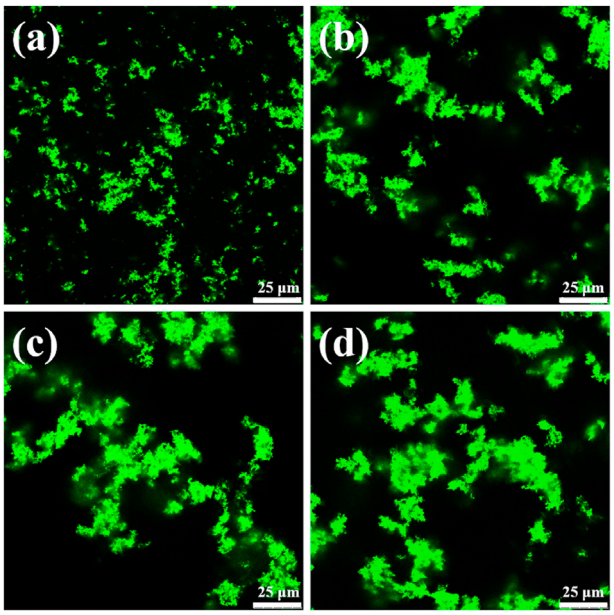

Fig. 3. CLSM images (scale bar = 25 μm) of the 1 wt % EYPN dispersions obtained at different pHs: (a) pH 5.0; (b) pH 4.0; (c) pH 3.0; (d) pH 2.0.

EYPN nanoparticles have satisfactory surface activity and can rapidly migrate to the air-water interface, thus effectively reducing the surface tension, especially during the initial adsorption process. A similar behavior was also observed in the adsorption behavior of EYPNs at the oil-water interface (Du et al., 2019).

Further, as expected, the adsorption of EYPNs at the air-water interface was affected by pH changes. As seen from Fig. 4a, for the interface stabilized by 0.1 wt% EYPNs, at and above pH 6.0, the systems exhibited similar adsorption kinetics and reached nearly identical surface tension values after 3 h (about 46 mN/m) (Fig. 4c), suggesting the interfaces formed at these pHs have similar surface density and composition. With the decrease of pH values, the EYPNs had higher interfacial adsorption with lower equilibrated surface tension values (Fig. 4c), which points to a higher surface activity. However, it should be noted that at pH 2.0 and 3.0, although the EYPNs had lower equilibrated surface tension, they showed higher initial surface tension values (1 s, 55.8–58.7 mN/m), indicating their slow initial adsorption at the interface. It is known that the initial adsorption kinetics of proteins and protein particles is generally limited by their diffusion from the bulk to the interface, which can be influenced by their size, shape, surface charge, as well as surface wettability (Wan, Yang, & Sagis, 2016a, 2016b; Wierenga et al., 2003; Mahmoudi et al., 2011). Therefore, we attributed the slow initial adsorption of EYPNs at pH 2.0 and 3.0 to the large size of formed particle clusters and aggregates (Fig. 1a–c), which thus hinder their fast diffusion to the interface. Once they have reached the interface, the lower equilibrated surface tension values were obtained since the electrostatic repulsion energy barrier for adsorption at these pHs is low (Fig. 1c). In contrast, as shown in Fig. 4b, at high EYPN concentration (1 wt%), the impact of pH changes on the initial surface tension values of EYPNs was not so obvious, mainly due to the sufficient surface-active materials at the interface during the initial adsorption. However, after 3 h of adsorption, the EYPNs at low pH values of 2.0–5.0 still showed lower equilibrated surface tension values (Fig. 4c), indicating their higher surface activity at these pHs due to the lower electrostatic adsorption barrier (Fig. 1c). In addition, due to the relatively high stability of EYPNs towards ionic strength (Fig. 1d), the changes of NaCl concentration did not significantly affect the adsorption kinetics of EYPNs (1 wt%) (Fig. S2).

The interfacial wettability of colloidal particles is believed to be a key factor in understanding their adsorption at the liquid interfaces and plays an important role in the preparation of emulsions and foams (Binks, 2002; Binks and Horozov, 2005; Dickinson et al., 2004). The wetting behaviors of EYPNs were studied by the measurements of air-in-water three-phase contact angles (θaw) on the dried EYPN substrate. Fig. 4d shows the effect of pH changes on the θaw values of EYPNs at different pHs. As can be seen, with the decrease of pH values, the θaw gradually increased and reached a maximum (54.7–56.6°) at pH 2.0 and 3.0. This suggests that the pH changes can significantly affect the interfacial wettability of EYPNs, and the increased hydrophobicity could be explained by the increased surface roughness of these heterogeneous

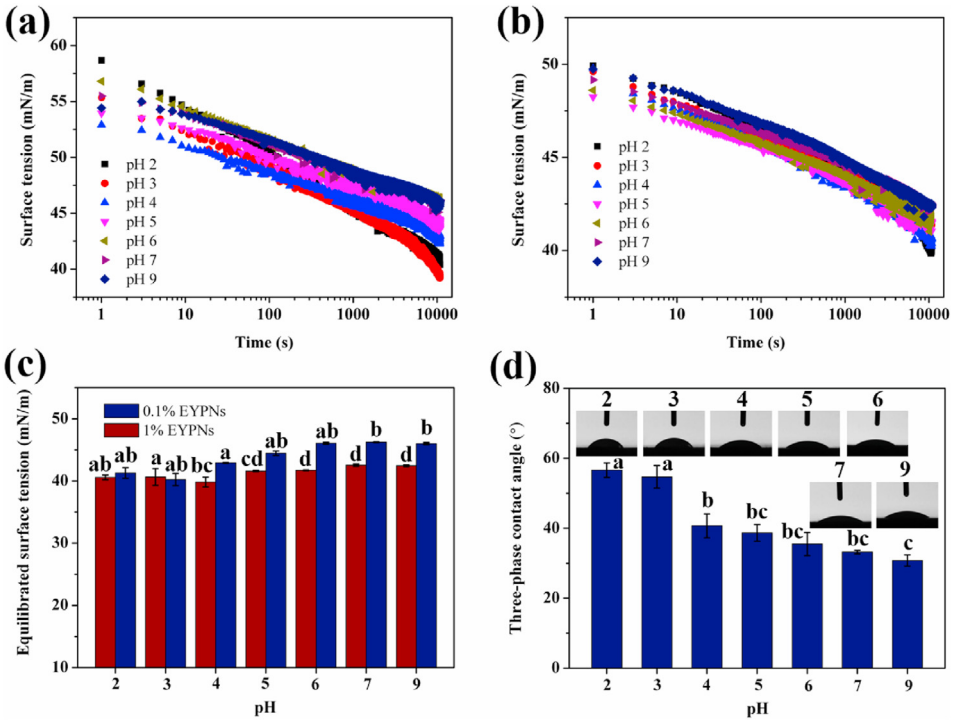

Fig. 4. (a and b) Surface tension as a function of time for EYPN dispersions (0.1 and 1 wt%) prepared at different pHs (2.0–9.0) at the air-water interface. Particle concentrations: (a) 0.1 wt%; (b) 1 wt%. (c) Equilibrated surface tension of these EYPNs (0.1 and 1 wt%). The equilibrated values represent the surface tension after 180 min of adsorption. (d) Air-in-water three-phase contact angles (θaw) of the EYPNs obtained at different pHs (2.0–9.0). Note: Different letters in each data of samples indicate significant differences between groups ($p < 0.05$).

nanoparticle clusters and aggregates formed at lower pH values (Figs. 1–3). Furthermore, the attachment energy (ΔG) of hydrophilic particles at the interface can be given by the equation: $\Delta G = \pi R^2\gamma(1- \cos\theta aw)^2$, where R is the nanoparticle radius and γ is the surface tension of the air-water interface formed from 1 wt% EYPNs. Thus, based on the experimental results, we can obtain a very high energy of around 100 kT for the attachment of EYPNs to the interface, which means that once at the interface, the EYPNs with intermediate hydrophobicity can be considered as an effective "irreversible adsorption" (Binks, 2002; Binks and Horozov, 2005), and thus can be used as a Pickering-type stabilizer to make aqueous foams.

3.3. Foaming properties of EYPNs

We employ these edible EYPNs as a Pickering-type particulate stabilizer for preparing aqueous foams to examine their macroscopic foaming behavior. Fig. 5a and b shows the effect of pH changes (2.0–9.0) on the formation and stability of foams generated from EYPN systems (1 wt%). As can be seen, all the samples had quite high foamability, as evidenced by the photographs of the foams immediately after aeration (Fig. 5b) as well as the high overruns (above 250%, see inset image of Fig. 5a), suggesting the formation of relatively wet foams. The high foamability of EYPNs is mainly due to the relatively high surface activity of these small EYPN nanoparticles (Fig. 4a and b), which can rapidly adsorb to the bubble surfaces during the mechanical shearing. With the decrease of pH values, the foam volume and overrun values gradually increased and then reached a maximum at pH 2.0 and 3.0, indicating the increased foamability. From the abovementioned results of adsorption kinetics (Fig. 4c), the EYPNs at low pH values had higher surface activity with lower equilibrated surface tension values, which thus contribute to the formation of air bubbles. Therefore, combining the dynamic surface tension measurements with the foamability results, we see a strong correlation between the interfacial adsorption behavior of EYPNs and their foamability.

The foam stability of all systems was then evaluated by measuring the foam volume with time. It can be clearly seen from Fig. 5a that the foam stability significantly increased with the decreasing pH values, and the foam stability of EYPNs at low pH values (2.0–4.0) was much higher than those at pH 5.0–9.0. This could be explained by the fact that at these low pHs, the EYPNs had higher surface activity (Fig. 4c), and there was less electrostatic repulsion between the adsorbed particles (Fig. 1c), both of which can contribute to the formation of the particle-laden interfaces with a higher packing density (Wan, Yang and Sagis, 2016a; Wierenga et al., 2005). The higher density of the adsorbed layer could provide stronger steric stabilization, thus increasing the foam stability. Additionally, some large particle clusters and aggregates formed at pH 2.0–4.0 may be entrapped inside the thin liquid films and the Plateau borders, which could solidify and stabilize the foam films and thus contribute to the foam stability by decreasing the liquid drainage, coalescence, and coarsening processes. These analyses can be supported by the following microstructure observations of foams (Figs. 6 and 7). Similar observations were also reported about the effect of the fractal and fibrillar aggregates from various proteins on their foaming properties (Wan, Yang and Sagis, 2016a; Fameau and Salonen, 2014; Fameau, & Salonen, 2014, 2014; Oboroceanu et al., 2014). We then further investigated the impact of particle concentration (1–10 wt%) on the formation and stability of foams formed from EYPNs at low pH of 3.0. As can be seen in Fig. 5c and d, although the effect of particle concentration on foam overruns was not obvious, the increase of particle concentration can significantly increase the foam stability as expected, and apparent bubbles and foams can still be observed after at least 5 days of storage at 25 °C. In addition, as seen from Fig. S3, the increase of NaCl concentration can also to some extent improve the foam stability of EYPN system (1 wt%, pH 7.0); however, the overall foaming properties were not obviously affected by the changes of NaCl concentration (0–500 mM), which is probably due to their relatively high stability towards ionic strength (Fig. 1d).

To gain more insight into the arrangement of EYPNs within the foam structure, the microstructure observations of foams stabilized by EYPNs were performed by using CLSM (Fig. 6) and FE-SEM (Fig. 7). Fig. 6 shows the CLSM images of the wet foams formed from the Nile Blue-labelled

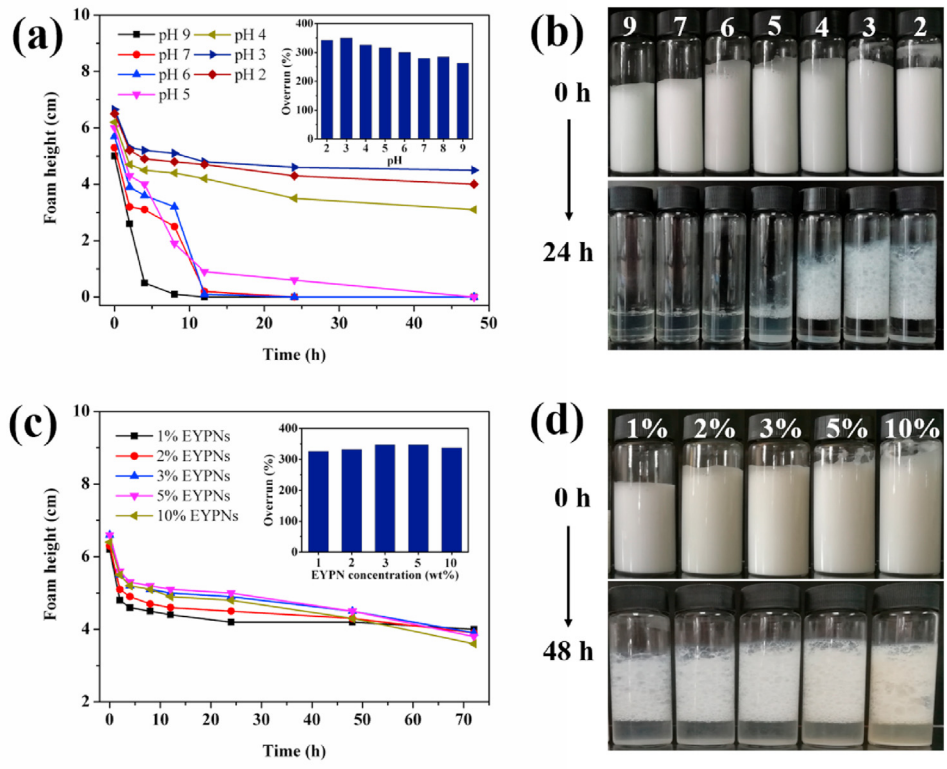

Fig. 5. (a and c) Foam height as a function of time at 25 °C for (a) the EYPN dispersions (1 wt %) prepared at different pHs (2.0–9.0) and (c) the EYPNs (pH 3.0) prepared with different particle concentrations (1–10 wt%). Inset images in (a) and (c) show the foam overruns of these samples. (b and d) Photographs of the foams generated from (b) the EYPNs (1 wt%) at different pHs (2.0–9.0) and (d) the EYPNs (pH 3.0) with different particle concentrations (1–10 wt%), taken at different time during storage at 25 °C.

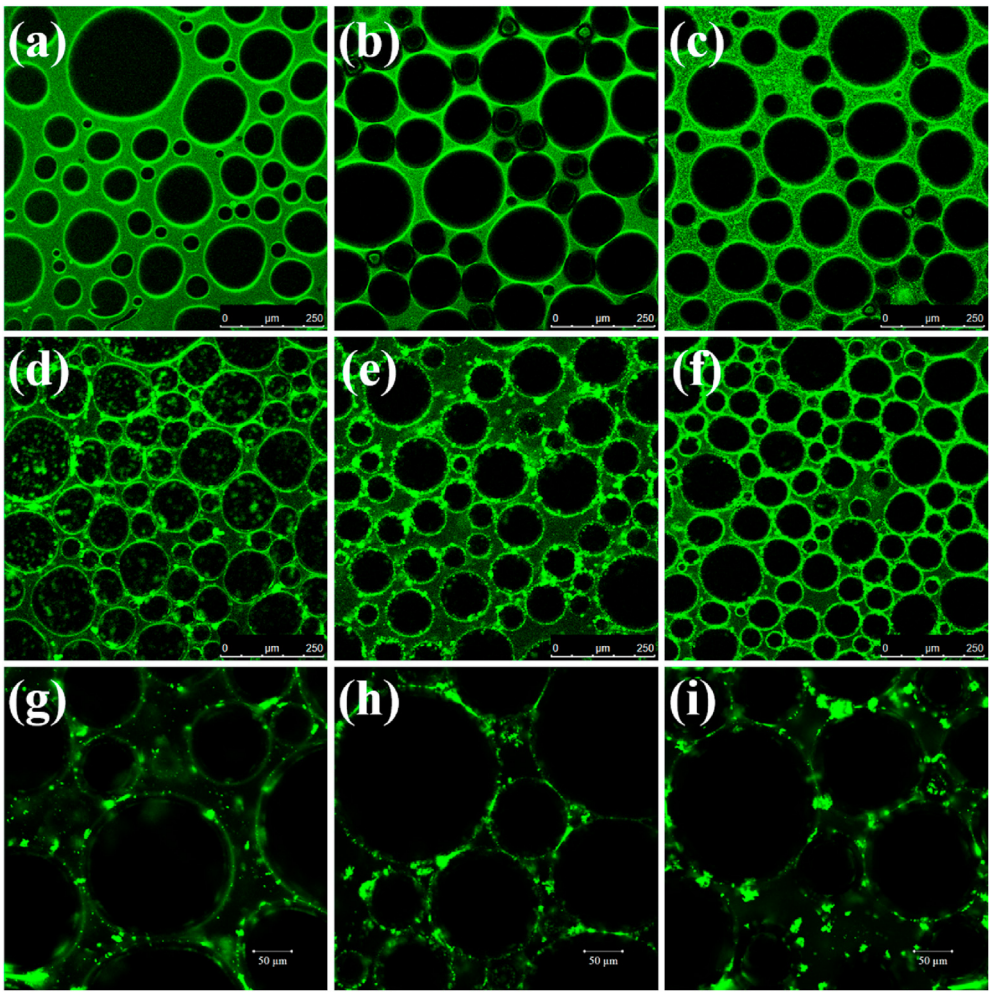

Fig. 6. CLSM images of initial foams prepared from the 1 wt % EYPNs at different pHs: (a) pH 9.0; (b) pH 7.0; (c) pH 5.0; (d and g) pH 4.0; (e and h) pH 3.0; (f and i) pH 2.0. The EYPNs were labelled with Nile Blue and are shown in green. Scale bars: (a–f) 250 μm; (g–i) 50 μm. (For interpretation of the references to colour in this figure legend, the reader is referred to the Web version of this article.)

EYPN systems at different pHs, obtained just after aeration. As can be seen, in all cases, the red fluorescent EYPN structures located around the surfaces of air bubbles as well as in the continuous phase of foams were clearly observed, confirming the formation of EYPN nanoparticle-stabilized bubbles and foams. With the decrease of pH values, the size of bubbles decreased with a more uniform bubble size distribution, which further confirms that the EYPNs at low pH values (2.0–5.0) had better foamability (Fig. 5a and b). At these low pHs (especially at pH 2.0–4.0), the obtained CLSM images clearly showed the adsorption and accumulation of particle aggregates at the bubble surfaces, which indicates that the EPYN aggregates and clusters can diffuse from the bulk to the interface, forming the interfacial aggregated particle structures. The anchorage of particle aggregates at the interface is believed to increase the elasticity of the adsorbed layer and thus can lead to an increase of the foam stability (Wan, Yang and Sagis, 2016a; Fameau and Salonen, 2014; Oboroceanu et al., 2014), as evidenced by the abovementioned foam stability (Fig. 5b). In addition, some large particle clusters and/or aggregates in the continuous phase of foams were also observed. These observations can be more clearly seen from the higher magnification CLSM images (Fig. 6g–i) of wet foams, as well as the FE-SEM images (Fig. 7) of dried foams, obtained at these low pHs. As can be seen in Fig. 7, the relatively smooth structures of bubble surfaces were observed for the foams at pH 7.0 (Fig. 7c and f) due to the fusion of small EYPNs during drying. In contrast, the SEM images obtained at pH 2.0 and 3.0 (Fig. 7a and b, d, and e) clearly confirmed the presence of large particle aggregates which are adsorbed to the air-water interface to stabilize air bubbles. This is further supported by the microstructure of dried foams (pH 3.0) by air-drying, where the adsorbed layer of particle aggregates on the bubble surfaces as well as the tightly aggregated particle chunks in the continuous phase were mainly observed (Fig. 7g–i). These observations are in good agreement with the results of aggregation behavior of EYPN dispersions (Figs. 1–3) as well as their macroscopic foaming behavior (Fig. 5).

4. Conclusions

In this work, we have studied the adsorption and foaming properties of an edible peptide-based colloidal nanoparticles, EYPNs, which show the potential as an efficient particulate stabilizer for development of food-grade aqueous foams. We examined the influence of particle aggregation behavior induced by the changes of environmental conditions (mainly the pH) on these properties of EYPN systems. The obtained results showed that the EYPNs are a highly pH-responsive system, and their aggregation in aqueous solutions strongly depend on the pH changes. At high pH values (6.0–9.0), the EYPNs are colloidally stable and negatively charged, whereas large particle clusters and/or aggregates were formed at low pH values (2.0–5.0) due to the reduced electrostatic repulsion forces. The pH-dependent particle aggregation behavior of EYPNs was found to have a significant effect on the interfacial adsorption and foaming properties of systems. Compared to high pH of 6.0–9.0, the

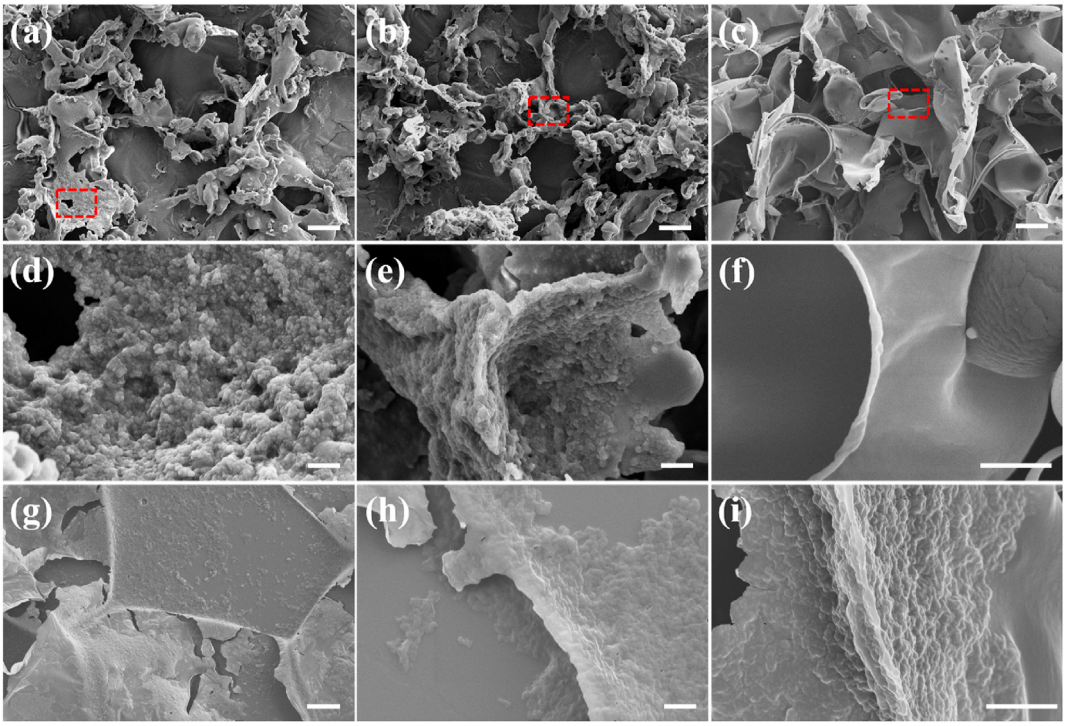

Fig. 7. FE-SEM images of the dried foams prepared from the 1 wt % EYPNs at different pHs: (a, d, g, and h) pH 2.0; (b, e, and i) pH 3.0; (c and f) pH 7.0. (d–f) Magnified images of selected area in images (a–c). The samples for SEM observations were obtained by (a–f) freeze drying and (g–i) air drying, respectively. Scale bars: (a–c) 10 μm; (d-f, h, and i) 1 μm; (g) 5 μm.

EYPNs at low pH (2.0–5.0) showed higher surface activity with a lower equilibrated surface tension, due to the reduced electrostatic adsorption barrier. In addition, the increased surface roughness of these heterogeneous particle clusters and aggregates formed at low pH led to the increased hydrophobicity of EYPNs. Accordingly, the foamability and foam stability of EYPNs at low pH values (2.0–4.0) were significantly higher than those at high pH of 5.0–9.0, which is mainly due to the higher surface activity and the formation of the particle-laden interfaces with a higher packing density at these low pHs. The presence of large particle clusters and aggregates in the continuous phase may also contribute to the foam stability of EYPN system. Additionally, the overall adsorption kinetics and foaming properties of EYPNs were not obviously affected by the changes of NaCl concentration, probably due to their relatively high stability towards ionic strength. These results indicate that our edible peptide-based nanoparticle EYPNs can be used as a new class of Pickering-type foam stabilizer for the development of food foams with controlled material properties, which are expected to have sustainable applications in food processing, cosmetics, and personal care products.

CRediT authorship contribution statement

Mengyue Xu: Investigation, Methodology, Formal analysis, Visualization, Writing – original draft. **Zhenya Du:** Investigation, Methodology, Formal analysis, Visualization, Writing – original draft. **Huanyin Liang:** Investigation, Formal analysis. **Yunyi Yang:** Investigation, Formal analysis. **Qing Li:** Investigation, Methodology, Formal analysis. **Zhili Wan:** Conceptualization, Methodology, Supervision, Project administration, Funding acquisition, Resources, Formal analysis, Writing – review & editing. **Xiaoquan Yang:** Conceptualization, Supervision, Funding acquisition.

Declaration of competing interest

The authors declare that they have no known competing financial interests or personal relationships that could have appeared to influence the work reported in this paper.

Acknowledgments

This work is supported by grants from the National Natural Science Foundation of China (No. 31801476), the Natural Science Foundation of Guangdong Province (Nos. 2021A1515011000 and 2018A030310409), the Fundamental Research Funds for the Central Universities (No. 2020ZYGXZR092), and the 111 Project (No. B17018).

Appendix A. Supplementary data

Supplementary data to this article can be found online at https://doi.org/10.1016/j.crfs.2021.04.002.

References

Alargova, R.G., Warhadpande, D.S., Paunov, V.N., Velev, O.D., 2004. Foam superstabilization by polymer microrods. Langmuir 20, 10371–10374.
Arriaga, L.R., Drenckhan, W., Salonen, A., Rodrigues, J.A., Íñiguez-Palomares, R., Rio, E., Langevin, D., 2012. On the long-term stability of foams stabilised by mixtures of nano-particles and oppositely charged short chain surfactants. Soft Matter 8, 11085–11097.
Asghari, A.K., Norton, I., Mills, T., Sadd, P., Spyropoulos, F., 2016. Interfacial and foaming characterisation of mixed protein-starch particle systems for food-foam applications. Food Hydrocolloids 53, 311–319.
Binks, B.P., 2002. Particles as surfactants-similarities and differences. Curr. Opin. Colloid Interface Sci. 7, 21–41.
Binks, B.P., Horozov, T.S., 2005. Aqueous foams stabilized solely by silica nanoparticles. Angew. Chem. Int. Ed. 44, 3722–3725.
Binks, B.P., Murakami, R., Armes, S.P., Fujii, S., Schmid, A., 2007. pH-responsive aqueous foams stabilized by ionizable latex particles. Langmuir 23, 8691–8694.
Binks, B.P., Kirkland, M., Rodrigues, J.A., 2008. Origin of stabilisation of aqueous foams in nanoparticle-surfactant mixtures. Soft Matter 4, 2373–2382.
Binks, B.P., Muijlwijk, K., Koman, H., Poortinga, A.T., 2017. Food-grade Pickering stabilisation of foams by in situ hydrophobisation of calcium carbonate particles. Food Hydrocolloids 63, 585–592.
Cantat, I., Cohen-Addad, S., Elias, F., Graner, F., Höhler, R., Pitois, O., Rouyer, F., Saint-Jalmes, A., 2013. Foams: Structure and Dynamics. Oxford University Press, Oxford.

Cervin, N.T., Andersson, L., Ng, J.B., Olin, P., Bergstrom, L., Wagberg, L., 2013. Lightweight and strong cellulose materials made from aqueous foams stabilized by nanofibrillated cellulose. Biomacromolecules 14, 503–511.
Cui, Z.G., Cui, Y.Z., Cui, C.F., Chen, Z., Binks, B.P., 2010. Aqueous foams stabilized by in situ surface activation of $CaCO_3$ nanoparticles via adsorption of anionic surfactant. Langmuir 26, 12567–12574.
Dai, L., Sun, C., Li, R., Mao, L., Liu, F., Gao, Y., 2017. Structural characterization, formation mechanism and stability of curcumin in zein-lecithin composite nanoparticles fabricated by antisolvent co-precipitation. Food Chem. 237, 1163–1171.
Dickinson, E., Kostakis, T., Murray, B.S., 2004. Factors controlling the formation and stability of air bubbles stabilized by partially hydrophobic silica nanoparticles. Langmuir 20, 8517–8525.
Dombrowski, J., Johler, F., Warncke, M., Kulozik, U., 2016. Correlation between bulk characteristics of aggregated β-lactoglobulin and its surface and foaming properties. Food Hydrocolloids 61, 318–328.
Du, Z., Bilbao-Montoya, M.P., Binks, B.P., Dickinson, E., Ettelaie, R., Murray, B.S., 2003. Outstanding stability of particle-stabilized bubbles. Langmuir 19, 3106–3108.
Du, Z., Li, Q., Li, J., Su, E., Liu, X., Wan, Z., Yang, X., 2019. Self-assembled egg yolk peptide micellar nanoparticles as a versatile emulsifier for food-grade oil-in-water Pickering nanoemulsions. J. Agric. Food Chem. 67, 11728–11740.
Fameau, A.-L., Salonen, A., 2014. Effect of particles and aggregated structures on the foam stability and aging. Compt. Rendus Phys. 15, 748–760.
Fujii, S., Iddon, P.D., Ryan, A.J., Armes, S.P., 2006. Aqueous particulate foams stabilized solely with polymer latex particles. Langmuir 22, 7512–7520.
Gonzenbach, U.T., Studart, A.R., Tervoort, E., Gauckler, L.J., 2006. Ultrastable particle-stabilized foams. Angew. Chem. Int. Ed. 45, 3526–3530.
Li, X., Murray, B.S., Yang, Y., Sarkar, A., 2020. Egg white protein microgels as aqueous Pickering foam stabilizers: bubble stability and interfacial properties. Food Hydrocolloids 98, 105292.
Maestro, A., Rio, E., Drenckhan, W., Langevin, D., Salonen, A., 2014. Foams stabilised by mixtures of nanoparticles and oppositely charged surfactants: relationship between bubble shrinkage and foam coarsening. Soft Matter 10, 6975–6983.
Mahmoudi, N., Axelos, M.A.V., Riaublanc, A., 2011. Interfacial properties of fractal and spherical whey protein aggregates. Soft Matter 7, 7643–7654.
Matsumiya, K., Murray, B.S., 2016. Soybean protein isolate gel particles as foaming and emulsifying agents. Food Hydrocolloids 60, 206–215.
Oboroceanu, D., Wang, L., Magner, E., Auty, M.A.E., 2014. Fibrillization of whey proteins improves foaming capacity and foam stability at low protein concentrations. J. Food Eng. 121, 102–111.
Peng, D., Jin, W., Tang, C., Lu, Y., Wang, W., Li, J., Li, B., 2018. Foaming and surface properties of gliadin nanoparticles: influence of pH and heating temperature. Food Hydrocolloids 77, 107–116.
Rio, E., Drenckhan, W., Salonen, A., Langevin, D., 2014. Unusually stable liquid foams. Adv. Colloid Interface Sci. 205, 74–86.
Schmitt, C., Bovay, C., Rouvet, M., Shojaei-Rami, S., Kolodziejczyk, E., 2007. Whey protein soluble aggregates from heating with NaCl physicochemical, interfacial, and foaming properties. Langmuir 23, 4155–4166.
Shen, P., Zhou, F., Zhang, Y., Yuan, D., Zhao, Q., Zhao, M., 2020. Formation and characterization of soy protein nanoparticles by controlled partial enzymatic hydrolysis. Food Hydrocolloids 105, 105844.
Wan, Z., Yang, X., Sagis, L.M.C., 2016a. Contribution of long fibrils and peptides to surface and foaming behavior of soy protein fibril system. Langmuir 32, 8092–8101.
Wan, Z.L., Guo, J., Yang, X.Q., 2015. Plant protein-based delivery systems for bioactive ingredients in foods. Food Funct. 6, 2876–2889.
Wan, Z., Yang, X., Sagis, L.M., 2016b. Nonlinear surface dilatational rheology and foaming behavior of protein and protein fibrillar aggregates in the presence of natural surfactant. Langmuir 32, 3679–3690.
Wierenga, P.A., Meinders, M.B.J., Egmond, M.R., Voragen, F.A.G.J., Jongh, H. H. J. De, 2003. Protein exposed hydrophobicity reduces the kinetic barrier for adsorption of ovalbumin to the air-water interface. Langmuir 19, 8964–8970.
Wierenga, P.A., Meinders, M.B.J., Egmond, M.R., Voragen, A.G.J., Jongh, H. H. J. de, 2005. Quantitative description of the relation between protein net charge and protein adsorption to air-water interfaces. J. Phys. Chem. B 109, 16946–16952.
Zhang, Z., Tan, H., Zhao, Y., Wang, Q., Wang, H., 2019. Facile synthesis of macroporous zwitterionic hydrogels templated from graphene oxide-stabilized aqueous foams. J. Colloid Interface Sci. 553, 40–49.
Zou, Y., Wan, Z., Guo, J., Wang, J., Yin, S., Yang, X., 2016. Modulation of the surface properties of protein particles by a surfactant for stabilizing foams. RSC Adv. 6, 66018–66026.